Robotica (2001) volume 19, pp. 11–19. Printed in the United Kingdom © 2001 Cambridge University Press

# PD control with feedforward compensation for robot manipulators: analysis and experimentation*

Victor Santibañez** and Rafael Kelly†

(Received in Final Form: May 15, 2000)


## SUMMARY

One of the simplest and natural appealing motion control strategies for robot manipulators is the PD control with feedforward compensation. Although successful experimental tests of this control scheme have been published since the beginning of the eighties, the proof of global asymptotic stability has remained unattended until now. The contribution of this paper is to prove that global asymptotic stability can be guaranteed provided that the proportional and derivative gains are adequately selected. The performance of the PD control with feedforward compensation evaluated on a two degrees-of-freedom direct-drive arm appears as fine as the classical model-based computed torque control scheme.


KEYWORDS: Motion control; Robot control; Stability analysis; Lyapunov function; PD control; Feedforward control

## 1. INTRODUCTION

The dynamics of a serial $n$-link rigid robot can be written as[1]

$$M(\boldsymbol{q})\ddot{\boldsymbol{q}}+C(\boldsymbol{q},\dot{\boldsymbol{q}})\dot{\boldsymbol{q}}+\boldsymbol{g}(\boldsymbol{q})=\tau \tag{1}$$

where $\boldsymbol{q}$ is the $n\times 1$ vector of joint displacements, $\dot{\boldsymbol{q}}$ is the $n\times 1$ vector of joint velocities, $\tau$ is the $n\times 1$ vector of applied torque inputs, $M(\boldsymbol{q})$ is the $n\times n$ symmetric positive definite manipulator inertia matrix, $C(\boldsymbol{q},\dot{\boldsymbol{q}})$ is the $n\times n$ matrix of centripetal and Coriolis torques, and $\boldsymbol{g}(\boldsymbol{q})$ is the $n\times 1$ vector of gravitational torques due to gravity.

The primary goal of motion control in joint space is to make the robot joints $\boldsymbol{q}$ track a given time-varying desired joint position $\boldsymbol{q}_d$. Rigorously, we say that the motion control objective in joint space is achieved provided that

$$\lim_{t\to\infty}\tilde{\boldsymbol{q}}(t)=\boldsymbol{0}$$

where $\tilde{\boldsymbol{q}}=\boldsymbol{q}_d-\boldsymbol{q}$ denotes the joint position error.

A number of control schemes for achieving this objective have been reported in the literature. This paper concerns with the PD control with feedforward compensation which is one of the simplest and natural appealing motion control scheme whose practical effectiveness has been reported since the early eighties. Despite this fact, at the best of the authors' knowledge, this control scheme lacks from the proof of global asymptotic stability. Since stability is a key requirement of control systems for application in the real world, we focus our attention – which is our main contribution – to provide such a stability analysis.

The PD control with feedforward compensation consists of a linear PD feedback plus a feedforward computation of the nominal robot dynamics (1) along the desired joint position trajectory. Thus, the control law can be written as

$$\tau=K_p\tilde{\boldsymbol{q}}+K_v\dot{\tilde{\boldsymbol{q}}}+M(\boldsymbol{q}_d)\ddot{\boldsymbol{q}}_d+C(\boldsymbol{q}_d,\dot{\boldsymbol{q}}_d)\dot{\boldsymbol{q}}_d+\boldsymbol{g}(\boldsymbol{q}_d) \tag{2}$$

where $K_p$ and $K_v$ are $n\times n$ diagonal positive definite matrices called the proportional and derivative gain matrices respectively. The desired joint position $\boldsymbol{q}_d$ is assumed to be twice continuously differentiable. The term "feedforward compensation" in the controller's name follows from the fact that the control law uses the robot dynamics explicitly evaluated at the desired motion.

Since the beginning of the eighties a number of studies of this controller have been reported in the literature. A brief summary of some of them is given here.

The PD control with feedforward compensation was suggested by Liégeois *et al.*[2] as an alternative to the on-line computation requirements of others model-based motion control schemes, particularly the computed torque control method. Experimental evaluations of this controller on direct-drive arms have been published since that time.

The first implementation of the PD control with feedforward compensation on a direct drive arm – the CMU Direct Drive Arm I – was reported in 1983 by Asada *et al.*[3] Further experiments and comparisons conducted on the CMU Direct-Drive Arm I were later described in the book by Asada and Youcef-Toumi.[4] The benefit of the feedforward compensation was concluded from such studies.

In 1986 An *et al.*[5] presented the results obtained from experiments of the PD control with feedforward compensation on the MIT Serial Link Direct Drive Arm. It was found that the tracking errors $\tilde{\boldsymbol{q}}$ decreased as more feedforward terms were considered. More experiments conducted on the MIT Serial Link Direct Drive Arm were described in the book by An *et al.*[6] References 6 and 7 presented experimental results using two model-based methods, namely, the PD control with feedforward compensation and the computed torque control. They concluded that both control schemes performed similarly and improved tracking accuracy significantly, when compared to independent joint PD control.

* Work partially supported by CONACyT grant No. 225080–5–32613A, CONACyT grant No. 411043–5–31948A, COSNET, and CYTED project: *Perception Systems for Robots*.
** Instituto Tecnológico de la Laguna, Apdo. Postal 49. Adm. 1, Torreón, Coah., 27001 (Mexico)
† División de Física Aplicada, CICESE, Apdo. Postal 2615, Adm. 1, Ensenada, B.C., 22800 (Mexico)

https://doi.org/10.1017/S0263574700002848 Published online by Cambridge University Press

Khosla and Kanade[8] compared the computed torque control scheme with the PD control plus feedforward compensation on the CMU Direct Drive Arm II. Also Khosla and Kanade[9] implemented the PD control showing best results for the model-based control techniques.

Evaluation on a network of transputers of the PD control plus feedforward compensation on a serial direct-drive arm was described by Chen *et al.*[10] A closed-chain direct-drive arm was used by Lu *et al.*[11] to implement four control algorithms including the PD control with feedforward compensation. The model-based control methods appeared as the best compared with the independent joint PD controller.

Beyond the evaluation of the PD control with feedforward compensation on direct-drive mechanisms, experiments on geared robots have been presented in the literature. Implementation of this controller on a COMAU industrial robot was described by Caccavale and Chiacchio.[12] In spite of the robot has high gear ratios at the joints, their experimental results demonstrate the performance improvement of the feedforward compensation with respect to the usual PID independent joint controller. Tarn *et al.*[13] presented experimental results on trajectory tracking performance of four servo schemes including the PD control with feedforward compensation on a PUMA 560 arm.

With reference to stability analysis considering the nonlinear robot dynamics (1), few studies have been reported. The first results were due to Wen and Bayard[14] and Wen.[15] They presented the study of a broad class of PD controllers including the PD control with feedforward compensation and conditions for asymptotic stability in a local sense were established. The study of this control system was also addressed in Kelly and Salgado[16] paying attention to conditions for ensuring equilibrium uniqueness and explicit conditions on the proportional and derivative gains for local asymptotic stability.

The theoretical contribution of this paper is the proof that the PD control with feedforward compensation is able to yield a globally asymptotically stable closed-loop system. The demonstration is carried out thanks to the concept of residual robot dynamics introduced by Arimoto in References 17 and 18 which is utilized here to derive a useful property related to growth rates as function of joint position and velocity.

This paper also discusses the experimental evaluation of the PD control with feedforward compensation on a two degrees-of-freedom vertical direct-drive robot arm. Because the direct-drive nature of the arm, the robot nonlinear dynamics cannot be neglected which is particularly true in our case where high speed motions are requested. The performance appears as fine as the classical model-based computed torque control scheme.

Throughout this paper, we use the notation $\lambda_{\mathrm{m}}\{A\}$ and $\lambda_{\mathrm{M}}\{A\}$ to indicate the smallest and largest eigenvalues, respectively, of a symmetric positive definite bounded matrix $A(\boldsymbol{x})$, for any $\boldsymbol{x} \in \mathbb{R}^n$. The norm of vector $\boldsymbol{x}$ is defined as $\|\boldsymbol{x}\| = \sqrt{\boldsymbol{x}^T\boldsymbol{x}}$ and that of matrix $A$ is defined as the corresponding induced norm $\|A\| = \sqrt{\lambda_{\mathrm{M}}\{A^TA\}}$.

This paper is organized as follows. Section 2 describes guidelines for selection of the controller gains. In Section 3 we present the closed-loop control system dynamics. The equilibrium uniqueness is treated in Section 4. Section 5 presents the main stability analysis. Section 6 describes the experimental study. Finally, we offer a brief summary in Section 7.

## 2. GUIDELINE FOR SELECTION OF GAINS

In this paper we assume that the robot links are jointed together with revolute joints, and upper bounds on the norm of the desired velocity and acceleration, denoted by $\|\dot{\boldsymbol{q}}_d\|_{\mathrm{M}}$ and $\|\ddot{\boldsymbol{q}}_d\|_{\mathrm{M}}$, are known.

The selection of the controller gains – proportional matrix $K_p$ and derivative matrix $K_v$ – depends obviously on the robot dynamics. Four parameters, denoted here by $k_M$, $k_{C1}$, $k_{C2}$ and $k_g$, associated to the inertia matrix $M(\boldsymbol{q})$, the centripetal and Coriolis matrix $C(\boldsymbol{q}, \dot{\boldsymbol{q}})$, and the gravitational torque vector $\boldsymbol{g}(\boldsymbol{q})$, respectively, are particularly important for this paper. They are defined such that[16]

$$\|M(\boldsymbol{x})\boldsymbol{z} - M(\boldsymbol{y})\boldsymbol{z}\| \leq k_M \|\boldsymbol{x} - \boldsymbol{y}\| \; \|\boldsymbol{z}\|, \tag{3}$$

$$\|C(\boldsymbol{x}, \boldsymbol{z})\boldsymbol{w} - C(\boldsymbol{y}, \boldsymbol{v})\boldsymbol{w}\| \leq k_{C1} \|\boldsymbol{z} - \boldsymbol{v}\| \; \|\boldsymbol{w}\| + k_{C2} \|\boldsymbol{z}\| \; \|\boldsymbol{x} - \boldsymbol{y}\| \; \|\boldsymbol{w}\| \tag{4}$$

$$\|\boldsymbol{g}(\boldsymbol{x}) - \boldsymbol{g}(\boldsymbol{y})\| \leq k_g \|\boldsymbol{x} - \boldsymbol{y}\|, \tag{5}$$

for all $\boldsymbol{v}, \boldsymbol{w}, \boldsymbol{x}, \boldsymbol{y}, \boldsymbol{z} \in \mathbb{R}^n$. Parameter $k_{C1}$ in (4) also satisfies

$$\|C(\boldsymbol{x},\boldsymbol{y})\boldsymbol{z}\| \leq k_{C1} \|\boldsymbol{y}\| \; \|\boldsymbol{z}\| \tag{6}$$

One way to compute these parameters is through[16]

$$k_M = n^2 \left[ \max_{i,\, j,\, k,\, \boldsymbol{q}} \left| \frac{\partial M_{ij}(\boldsymbol{q})}{\partial q_k} \right| \right], \tag{7}$$

$$k_{C1} = n^2 \left[ \max_{i,\, j,\, k,\, \boldsymbol{q}} \left| c_{ijk}(\boldsymbol{q}) \right| \right], \tag{8}$$

$$k_{C2} = n^3 \left[ \max_{i,\, j,\, k,\, l,\, \boldsymbol{q}} \left| \frac{\partial c_{ijk}(\boldsymbol{q})}{\partial q_l} \right| \right], \tag{9}$$

$$k_g = n \left[ \max_{i,\, j,\, \boldsymbol{q}} \left| \frac{\partial g_i(\boldsymbol{q})}{\partial q_j} \right| \right], \tag{10}$$

where $M_{ij}(\boldsymbol{q})$ is the $ij$-element of matrix $M(\boldsymbol{q})$, $c_{ijk}(\boldsymbol{q})$ is the $ijk$ Christoffel symbol, and $g_i(\boldsymbol{q})$ is the $i$-element of vector $\boldsymbol{g}(\boldsymbol{q})$.

Let us digress momentarily to define the positive parameters $k_1$, and $k_2$ such that

$$\|\boldsymbol{g}(\boldsymbol{x})\| \leq k_1, \tag{11}$$

$$\|M(\boldsymbol{x})\boldsymbol{z}\| \leq k_2\|\boldsymbol{z}\|, \tag{12}$$

for all $\boldsymbol{x}, \boldsymbol{z} \in \mathbb{R}^n$. Parameters $k_1$ and $k_2$ always exist because the assumption that the manipulator joints are revolute, then $\boldsymbol{g}(\boldsymbol{q})$ and $M(\boldsymbol{q})$ are bounded.

In this paper we propose the selection of gain matrices $K_p$ and $K_v$ according to the following simple guidelines concerning their smallest eigenvalues:

https://doi.org/10.1017/S0263574700002848 Published online by Cambridge University Press

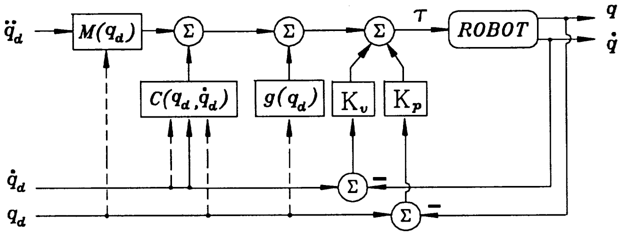


Fig. 1. PD control with feedforward compensation.

$$\lambda_{\mathrm{m}}\{K_p\} >> k_g + k_M \|\ddot{\boldsymbol{q}}_d\|_{\mathrm{M}} + k_{C2}\|\dot{\boldsymbol{q}}_d\|^2_{\mathrm{M}}, \tag{13}$$

$$\lambda_{\mathrm{m}}\{K_v\} > k_{C1}\|\dot{\boldsymbol{q}}_d\|_{\mathrm{M}}. \tag{14}$$

Under these conditions, – more detailed expressions will be provided later on – the control system is globally asymptotically stable as will be established in Section 5.

It should be emphasized that conditions (13) and (14) impose the gain matrices $K_p$ and $K_v$ to be large enough – but finite – as a requirement to get asymptotic stability in a global sense. As a quantitative overcome, the computation of matrices $K_p$ and $K_v$ in agreement with (13) and (14) respectively, requires knowledge of the following parameters related to the robot dynamics: $k_M$, $k_{C1}$, $k_{C2}$, $k_g$, $k_1$ and $k_2$.

## 3. CLOSED-LOOP SYSTEM

The overall closed-loop system, whose block diagram is depicted in Figure 1, is obtained by substituting the control law (2) into the robot dynamics (1). This gives the following nonautonomous nonlinear differential equation written in terms of the state vector $[\tilde{\boldsymbol{q}}^T \; \dot{\tilde{\boldsymbol{q}}}^T]^T$

$$\frac{d}{dt}\begin{bmatrix} \tilde{\boldsymbol{q}} \\ \dot{\tilde{\boldsymbol{q}}} \end{bmatrix} = \begin{bmatrix} \dot{\tilde{\boldsymbol{q}}} \\ M(\boldsymbol{q})^{-1}[-K_p\tilde{\boldsymbol{q}} - K_v\dot{\tilde{\boldsymbol{q}}} - C(\boldsymbol{q},\dot{\boldsymbol{q}})\dot{\tilde{\boldsymbol{q}}} - \boldsymbol{h}(\tilde{\boldsymbol{q}}, \dot{\tilde{\boldsymbol{q}}})] \end{bmatrix} \tag{15}$$

where

$$\boldsymbol{h}(\tilde{\boldsymbol{q}}, \dot{\tilde{\boldsymbol{q}}}) = [M(\boldsymbol{q}_d) - M(\boldsymbol{q})]\ddot{\boldsymbol{q}}_d + [C(\boldsymbol{q}_d, \dot{\boldsymbol{q}}_d) - C(\boldsymbol{q}, \dot{\boldsymbol{q}})]\,\dot{\boldsymbol{q}}_d + \boldsymbol{g}(\boldsymbol{q}_d) - \boldsymbol{g}(\boldsymbol{q}). \tag{16}$$

is the so-called residual robot dynamics introduced by Arimoto.[17,18]

We can easily check that the origin $[\tilde{\boldsymbol{q}}^T \; \dot{\tilde{\boldsymbol{q}}}^T]^T = \boldsymbol{0} \in \mathbb{R}^{2n}$ of the state space is an equilibrium regardless gain matrices $K_p$ and $K_v$. However, the number of equilibria for the closed-loop system (15) depends on the proportional gain $K_p$.[16]

The residual robot dynamics (16) possesses one notable property useful to prove equilibrium uniqueness and globality in the stability analysis. By defining

$$\alpha = 2\,\frac{k_1 + k_2\|\ddot{\boldsymbol{q}}_d\|_{\mathrm{M}} + k_{C1}\|\dot{\boldsymbol{q}}_d\|^2_{\mathrm{M}}}{\delta} \tag{17}$$

and

$$\delta = k_g + k_M\|\ddot{\boldsymbol{q}}_d\|_{\mathrm{M}} + k_{C2}\|\dot{\boldsymbol{q}}_d\|^2_{\mathrm{M}} \tag{18}$$

the norm of the residual dynamics (16) satisfies (see appendix A):

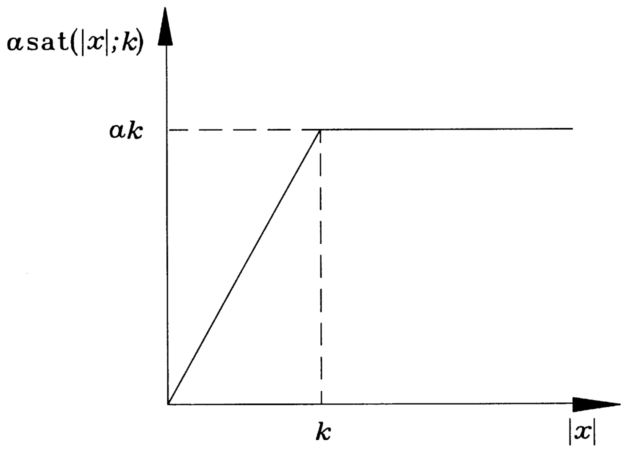


Fig. 2. Saturation function.

$$\|\boldsymbol{h}(\tilde{\boldsymbol{q}}, \dot{\tilde{\boldsymbol{q}}})\| \le k_{C1}\|\dot{\boldsymbol{q}}_d\|_{\mathrm{M}}\|\dot{\tilde{\boldsymbol{q}}}\| + \delta \;\mathrm{sat}(\|\tilde{\boldsymbol{q}}\|;\, \alpha) \tag{19}$$

where the hard saturation function $\mathrm{sat}(x;k)$ for $k>0$ depicted in Figure 2 is defined by:

$$\mathrm{sat}(x;\,k) = \begin{cases} x & \text{if } |x| \le k \\ k & \text{if } x > k \\ -k & \text{if } x < -k \end{cases} \tag{20}$$

The main contribution of this paper is to provide conditions on gain matrices $K_p$ and $K_v$ to guarantee that, the point $[\tilde{\boldsymbol{q}}^T \; \dot{\tilde{\boldsymbol{q}}}^T]^T = \boldsymbol{0} \in \mathbb{R}^{2n}$ is the unique equilibrium of the closed-loop system (15), and it is globally asymptotically stable. The next sections are devoted to demonstrate such statement.

## 4. EQUILIBRIUM UNIQUENESS

The equilibria of the closed-loop equation (15) are the constant vectors $[\tilde{\boldsymbol{q}}^T \; \dot{\tilde{\boldsymbol{q}}}^T]^T = [\boldsymbol{s}^T \; \boldsymbol{0}^T]^T \in \mathbb{R}^{2n}$, where $\boldsymbol{s} \in \mathbb{R}^n$ is a solution of

$$K_p\boldsymbol{s} + \boldsymbol{h}(\boldsymbol{s},\, \boldsymbol{0}) = \boldsymbol{0}. \tag{21}$$

Above equation always has the trivial solution $\boldsymbol{s} = \boldsymbol{0} \in \mathbb{R}^n$, but some others $\boldsymbol{s}$ may also be solutions, depending obviously on $K_p$. Explicit conditions on the proportional gain to ensure uniqueness of this equilibrium were first reported in Reference 16. Next, we provide an alternative way to derive such a condition by invoking the contraction mapping theorem. To this end, let us define

$$\boldsymbol{k}(\boldsymbol{s}) = K_p^{-1}\boldsymbol{h}(\boldsymbol{s},\, \boldsymbol{0}).$$

The idea is to note that any fixed point $\boldsymbol{s} \in \mathbb{R}^n$ of $\boldsymbol{k}(\boldsymbol{s})$ is a solution of (21). Thus, we are interested in finding conditions on $K_p$ such that $\boldsymbol{k}(\boldsymbol{s})$ has a unique fixed point. Since $\boldsymbol{s} = 0$ is always a fixed point, then it will be the unique one.

Notice that for all $\boldsymbol{x}, \boldsymbol{y} \in \mathbb{R}^n$, we have

$$\begin{aligned} \|\boldsymbol{k}(\boldsymbol{x}) - \boldsymbol{k}(\boldsymbol{y})\| &\le \|K_p^{-1}[\boldsymbol{h}(\boldsymbol{x}, 0) - \boldsymbol{h}(\boldsymbol{y}, 0)]\| \\ &\le \lambda_{\mathrm{M}}\{K_p^{-1}\}\,\|\boldsymbol{h}(\boldsymbol{x}, 0) - \boldsymbol{h}(\boldsymbol{y}, 0)\|. \end{aligned}$$

In view of (19), it can be shown that

$$\|\boldsymbol{h}(\boldsymbol{x},0) - \boldsymbol{h}(\boldsymbol{y},0)\| \le \delta\,\mathrm{sat}(\|\boldsymbol{x} - \boldsymbol{y}\|;\, \alpha).$$

Hence, using $\lambda_{\mathrm{M}}\{K_p^{-1}\} = 1/\lambda_{\mathrm{m}}\{K_p\}$ (because $K_p$ is a symmetric positive definite matrix) we get

https://doi.org/10.1017/S0263574700002848 Published online by Cambridge University Press

$$\|\boldsymbol{k}(\boldsymbol{x})-\boldsymbol{k}(\boldsymbol{y})\| \leq \frac{\delta}{\lambda_{\mathrm{m}}\{K_p\}}\mathrm{sat}(\|\boldsymbol{x}-\boldsymbol{y}\|;\,\alpha)$$

$$\leq \frac{\delta}{\lambda_{\mathrm{m}}\{K_p\}}\|\boldsymbol{x}-\boldsymbol{y}\|.$$

Finally, by invoking the contraction mapping theorem, we conclude that

$$\lambda_{\mathrm{m}}\{K_p\} > \delta = k_g + k_M\|\ddot{\boldsymbol{q}}_d\|_{\mathrm{M}} + k_{C2}\|\dot{\boldsymbol{q}}_d\|^2_{\mathrm{M}}$$

is a sufficient condition for $\boldsymbol{k}(\boldsymbol{s})$ to have a unique fixed point, therefore, for the origin of the state space to be the unique equilibrium of the closed-loop system (15).

## 5. STABILITY ANALYSIS

The stability study of the trivial equilibrium of the closed-loop system (15) has been reported by several authors resulting in local asymptotic stability.[14–16] Below, we will present the analysis to prove asymptotic stability but in a global sense.

To this end we propose the following Lyapunov function candidate:

$$V(\tilde{\boldsymbol{q}},\dot{\tilde{\boldsymbol{q}}}) = \frac{1}{2}\dot{\tilde{\boldsymbol{q}}}^T M(\boldsymbol{q})\dot{\tilde{\boldsymbol{q}}} + \frac{1}{2}\tilde{\boldsymbol{q}}^T K_p\tilde{\boldsymbol{q}} + \varepsilon \boldsymbol{f}(\tilde{\boldsymbol{q}})^T M(\boldsymbol{q})\dot{\tilde{\boldsymbol{q}}} \tag{22}$$

where function $\boldsymbol{f}(\tilde{\boldsymbol{q}})$ is defined by

$$\boldsymbol{f}(\tilde{\boldsymbol{q}}) = \delta\frac{\alpha}{\tanh(\alpha\sigma)}\begin{bmatrix}\tanh(\sigma\tilde{q}_1)\\ \vdots \\ \tanh(\sigma\tilde{q}_n)\end{bmatrix}. \tag{23}$$

Parameters $\sigma$ in (23) and $\varepsilon$ in (22) are small positive constants satisfying

$$\frac{\tanh(\alpha\sigma)}{\alpha\sigma\sqrt{\delta\lambda_{\mathrm{M}}\{M\}}} \geq \varepsilon. \tag{24}$$

Several characteristics of $\boldsymbol{f}(\tilde{\boldsymbol{q}})$ are fundamental in the stability analysis. They are established in the following

***Lemma***. Function $\boldsymbol{f}(\tilde{\boldsymbol{q}})$ satisfies the following four inequalities:

$$\|\boldsymbol{f}(\tilde{\boldsymbol{q}})\| \geq \delta\,\mathrm{sat}(\|\tilde{\boldsymbol{q}}\|;\,\alpha), \tag{25}$$

$$\|\boldsymbol{f}(\tilde{\boldsymbol{q}})\| \leq \delta\frac{\alpha\sigma}{\tanh(\alpha\sigma)}\|\tilde{\boldsymbol{q}}\|, \tag{26}$$

$$\|\boldsymbol{f}(\tilde{\boldsymbol{q}})\|^2 \leq \delta\frac{\alpha\sigma}{\tanh(\alpha\sigma)}\boldsymbol{f}(\tilde{\boldsymbol{q}})^T\tilde{\boldsymbol{q}}, \tag{27}$$

$$\|\boldsymbol{f}(\tilde{\boldsymbol{q}})\| \leq \sqrt{n}\,\delta\frac{\alpha}{\tanh(\alpha\sigma)}. \tag{28}$$

***Proof***. Notice that

$$\|\boldsymbol{f}(\boldsymbol{q})\|^2 = \delta^2\frac{\alpha^2}{\tanh^2(\alpha\sigma)}\Big[|\tanh(\sigma\tilde{q}_1)|^2 + \cdots + |\tanh(\sigma\tilde{q}_n)|^2\Big]. \tag{29}$$

Inequality (25) follows from

$$\left|\delta\frac{\alpha}{\tanh(\alpha\sigma)}\tanh(\sigma\tilde{q}_i)\right| \geq \delta\,\mathrm{sat}(|\tilde{q}_i|;\,\alpha)$$

which holds for all $\tilde{q}_i \in \mathbb{R}$. Using the fact that $|\tanh(\sigma x)| \leq \sigma|x|$ for $x \in \mathbb{R}$, then we obtain any of inequalities (26) and (27). Finally, because $|\tanh(\sigma x)| \leq 1$ for $x \in \mathbb{R}$, from (29) we get (28).

□□□

The next subsections are devoted to show that gains $K_p$ and $K_v$ in (13) and (14), respectively, guarantee the global positiveness of $V(\tilde{\boldsymbol{q}},\dot{\tilde{\boldsymbol{q}}})$ and the global negativeness of its time derivative $\dot{V}(\tilde{\boldsymbol{q}},\dot{\tilde{\boldsymbol{q}}})$.

### 5.1 *Positiveness*

To show that the Lyapunov function candidate (22) is radially unbounded and positive definite we rewrite it as

$$V(\tilde{\boldsymbol{q}},\dot{\tilde{\boldsymbol{q}}}) = \frac{1}{2}[\dot{\boldsymbol{q}} + \varepsilon\boldsymbol{f}(\tilde{\boldsymbol{q}})]^T M(\boldsymbol{q})[\dot{\boldsymbol{q}} + \varepsilon\boldsymbol{f}(\tilde{\boldsymbol{q}})]$$

$$+\frac{1}{2}\tilde{\boldsymbol{q}}^T K_p\tilde{\boldsymbol{q}} - \frac{\varepsilon^2}{2}\boldsymbol{f}^T(\tilde{\boldsymbol{q}})M(\boldsymbol{q})\boldsymbol{f}(\tilde{\boldsymbol{q}}), \tag{30}$$

thus, it will be a radially unbounded positive definite function provided that

$$\frac{1}{2}\tilde{\boldsymbol{q}}^T K_p\tilde{\boldsymbol{q}} - \frac{\varepsilon^2}{2}\boldsymbol{f}^T(\tilde{\boldsymbol{q}})M(\boldsymbol{q})\boldsymbol{f}(\tilde{\boldsymbol{q}})$$

is also a radially unbounded positive definite function with respect to $\tilde{\boldsymbol{q}}$. To this end, first notice that

$$\frac{1}{2}\tilde{\boldsymbol{q}}^T K_p\tilde{\boldsymbol{q}} - \frac{\varepsilon^2}{2}\boldsymbol{f}^T(\tilde{\boldsymbol{q}})M(\boldsymbol{q})\boldsymbol{f}(\tilde{\boldsymbol{q}}) \geq \frac{\lambda_{\mathrm{m}}\{K_p\}}{2}\|\tilde{\boldsymbol{q}}\|^2$$

$$-\frac{\varepsilon^2\lambda_{\mathrm{M}}\{M\}}{2}\|\boldsymbol{f}(\tilde{\boldsymbol{q}})\|^2.$$

Since $\|\boldsymbol{f}(\tilde{\boldsymbol{q}})\|$ satisfies (26), then

$$\frac{1}{2}\tilde{\boldsymbol{q}}^T K_p\tilde{\boldsymbol{q}} - \frac{\varepsilon^2}{2}\boldsymbol{f}^T(\tilde{\boldsymbol{q}})M(\boldsymbol{q})\boldsymbol{f}(\tilde{\boldsymbol{q}})$$

$$\geq \frac{1}{2}\left[\lambda_{\mathrm{m}}\{K_p\} - \varepsilon^2\lambda_{\mathrm{M}}\{M\}\,\delta^2\frac{\alpha^2\sigma^2}{\tanh^2(\alpha\sigma)}\right]\|\tilde{\boldsymbol{q}}\|^2$$

which imposes

$$\lambda_{\mathrm{m}}\{K_p\} > \varepsilon^2\lambda_{\mathrm{M}}\{M\}\,\delta^2\frac{\alpha^2\sigma^2}{\tanh^2(\alpha\sigma)}$$

as a sufficient condition for positiveness of $V(\tilde{\boldsymbol{q}},\dot{\tilde{\boldsymbol{q}}})$. In virtue of definition of $\varepsilon$ in (24), the above condition is satisfied if

$$\lambda_{\mathrm{m}}\{K_p\} > k_g + k_M\|\ddot{\boldsymbol{q}}_d\|_{\mathrm{M}} + k_{C2}\|\dot{\boldsymbol{q}}_d\|^2_{\mathrm{M}}$$

which is implied by (13). In sum, we have the Lyapunov function candidate (22) is a radially unbounded and globally positive definite function.

### 5.2 Time derivative

The time derivative of the Lyapunov function candidate (22) along the trajectories of the closed loop equation (15) can be written as

$$\dot V(\tilde{\boldsymbol q},\dot{\tilde{\boldsymbol q}})=\dot{\tilde{\boldsymbol q}}^T\Big[-K_p\tilde{\boldsymbol q}-\boldsymbol K_v\dot{\tilde{\boldsymbol q}}-C(\boldsymbol q,\dot{\boldsymbol q})\dot{\tilde{\boldsymbol q}}-\boldsymbol h(\tilde{\boldsymbol q},\dot{\tilde{\boldsymbol q}})\Big]$$
$$+\frac{1}{2}\dot{\tilde{\boldsymbol q}}^T\dot M(\boldsymbol q)\dot{\tilde{\boldsymbol q}}$$
$$+\dot{\tilde{\boldsymbol q}}^TK_p\tilde{\boldsymbol q}+\varepsilon\dot{\boldsymbol f}(\tilde{\boldsymbol q})^TM(\boldsymbol q)\dot{\tilde{\boldsymbol q}}+\varepsilon\boldsymbol f(\tilde{\boldsymbol q})^T\dot M(\boldsymbol q)\dot{\tilde{\boldsymbol q}}$$
$$+\varepsilon\boldsymbol f(\tilde{\boldsymbol q})^T\Big[-K_p\tilde{\boldsymbol q}-K_v\dot{\tilde{\boldsymbol q}}-C(\boldsymbol q,\dot{\boldsymbol q})\dot{\tilde{\boldsymbol q}}-\boldsymbol h(\tilde{\boldsymbol q},\dot{\tilde{\boldsymbol q}})\Big].$$

If the matrix $C(\boldsymbol q,\dot{\boldsymbol q})$ is defined using the Christoffel symbol, then $\frac{1}{2}\dot M(\boldsymbol q)-C(\boldsymbol q,\dot{\boldsymbol q})$ is skew-symmetric, and $\dot M(\boldsymbol q)=C(\boldsymbol q,\dot{\boldsymbol q})+C(\boldsymbol q,\dot{\boldsymbol q})^T$ for all $\boldsymbol q,\dot{\boldsymbol q}\in\mathbb{R}^n$ (see e.g. Reference 19). Thanks to these expressions, the time derivative of the Lyapunov function becomes

$$\dot V(\tilde{\boldsymbol q},\dot{\tilde{\boldsymbol q}})=-\dot{\tilde{\boldsymbol q}}^TK_v\dot{\tilde{\boldsymbol q}}+\varepsilon\dot{\boldsymbol f}(\tilde{\boldsymbol q})^TM(\boldsymbol q)\dot{\tilde{\boldsymbol q}}-\varepsilon\boldsymbol f(\tilde{\boldsymbol q})^TK_p\tilde{\boldsymbol q}$$
$$-\varepsilon\boldsymbol f(\tilde{\boldsymbol q})^TK_v\dot{\tilde{\boldsymbol q}}+\varepsilon\boldsymbol f(\tilde{\boldsymbol q})^TC(\boldsymbol q,\dot{\boldsymbol q})^T\dot{\tilde{\boldsymbol q}}$$
$$-\dot{\tilde{\boldsymbol q}}^T\boldsymbol h(\tilde{\boldsymbol q},\dot{\tilde{\boldsymbol q}})-\varepsilon\boldsymbol f(\tilde{\boldsymbol q})^T\boldsymbol h(\tilde{\boldsymbol q},\dot{\tilde{\boldsymbol q}}).\qquad(31)$$

Since we look at upper bound $\dot V(\tilde{\boldsymbol q},\dot{\tilde{\boldsymbol q}})$ by a negative definite function in terms of the state vector, it is convenient to find upper bounds on each term of (31), particularly those involving $\varepsilon$.

At this point, note that the following inequality hold because $K_p$ is diagonal and positive definite

$$\varepsilon\boldsymbol f(\tilde{\boldsymbol q})^TK_p\tilde{\boldsymbol q}\geq\varepsilon\lambda_{\mathrm m}\{K_p\}\boldsymbol f(\tilde{\boldsymbol q})^T\tilde{\boldsymbol q}.$$

But using (27) dealing with $\boldsymbol f(\tilde{\boldsymbol q})^T\tilde{\boldsymbol q}$ we obtain

$$\varepsilon\boldsymbol f(\tilde{\boldsymbol q})^TK_p\tilde{\boldsymbol q}\geq\frac{\varepsilon\lambda_{\mathrm m}\{K_p\}}{\delta}\frac{\tanh(\alpha\sigma)}{\alpha\sigma}\|\boldsymbol f(\tilde{\boldsymbol q})\|^2$$

which finally yields the key inequality

$$-\varepsilon\boldsymbol f(\tilde{\boldsymbol q})^TK_p\tilde{\boldsymbol q}\leq-\frac{\varepsilon\lambda_{\mathrm m}\{K_p\}}{\delta}\frac{\tanh(\alpha\sigma)}{\alpha\sigma}\|\boldsymbol f(\tilde{\boldsymbol q})\|^2.\qquad(32)$$

The second term of (31) can be upper bounded as

$$\varepsilon\dot{\boldsymbol f}(\tilde{\boldsymbol q})^TM(\boldsymbol q)\dot{\tilde{\boldsymbol q}}\leq\varepsilon\lambda_{\mathrm M}\{M\}\delta\frac{\alpha\sigma}{\tanh(\alpha\sigma)}\|\dot{\tilde{\boldsymbol q}}\|^2\qquad(33)$$

where we have used the fact that $|\frac{d}{dt}\tanh(\sigma\tilde q_i)|=|\sigma\mathrm{sech}^2(\sigma\tilde q_i)\dot{\tilde q}_i|\leq\sigma|\dot{\tilde q}_i|$.

A straightforward bound on $-\varepsilon\boldsymbol f(\tilde{\boldsymbol q})^TK_v\tilde{\boldsymbol q}$ is given by

$$-\varepsilon\boldsymbol f(\tilde{\boldsymbol q})^TK_v\tilde{\boldsymbol q}\leq\varepsilon\lambda_{\mathrm M}\{K_v\}\left\|\dot{\tilde{\boldsymbol q}}\right\|\|\boldsymbol f(\tilde{\boldsymbol q})\|.\qquad(34)$$

The upper bound on the term $\varepsilon\boldsymbol f(\tilde{\boldsymbol q})^TC(\boldsymbol q,\dot{\boldsymbol q})^T\dot{\tilde{\boldsymbol q}}$ should be carefully selected. Notice that

$$\varepsilon\boldsymbol f(\tilde{\boldsymbol q})^TC(\boldsymbol q,\dot{\boldsymbol q})^T\dot{\tilde{\boldsymbol q}}=\varepsilon\dot{\tilde{\boldsymbol q}}^TC(\boldsymbol q,\dot{\boldsymbol q})\boldsymbol f(\tilde{\boldsymbol q})$$
$$\leq\varepsilon\|\dot{\tilde{\boldsymbol q}}\|\,\|C(\boldsymbol q,\dot{\boldsymbol q})\boldsymbol f(\tilde{\boldsymbol q})\|.$$

Considering the upper bound on $C(\boldsymbol q,\dot{\boldsymbol q})$ stated in (6), and $\|\dot{\boldsymbol q}\|=\|\dot{\boldsymbol q}_d-\dot{\tilde{\boldsymbol q}}\|\leq\|\dot{\boldsymbol q}_d\|+\|\dot{\tilde{\boldsymbol q}}\|$, it follows that

$$\varepsilon\boldsymbol f(\tilde{\boldsymbol q})^TC(\boldsymbol q,\dot{\boldsymbol q})^T\dot{\tilde{\boldsymbol q}}\leq\varepsilon k_{C1}\|\dot{\boldsymbol q}_d\|_{\mathrm M}\left\|\dot{\tilde{\boldsymbol q}}\right\|\|\boldsymbol f(\tilde{\boldsymbol q})\|+\varepsilon k_{C1}\left\|\dot{\tilde{\boldsymbol q}}\right\|^2\|\boldsymbol f(\tilde{\boldsymbol q})\|.$$

Hence, plugging (28) into the second right hand side term we finally obtain

$$\varepsilon\boldsymbol f(\tilde{\boldsymbol q})^TC(\boldsymbol q,\dot{\boldsymbol q})^T\dot{\tilde{\boldsymbol q}}\leq\varepsilon k_{C1}\|\dot{\boldsymbol q}_d\|_{\mathrm M}\|\dot{\tilde{\boldsymbol q}}\|\,\|\boldsymbol f(\tilde{\boldsymbol q})\|$$
$$+\varepsilon k_{C1}\sqrt{n}\,\delta\frac{\alpha}{\tanh(\alpha\sigma)}\|\dot{\tilde{\boldsymbol q}}\|^2.\qquad(35)$$

At this stage it remains to find upper bounds on the two terms involving $\boldsymbol h(\tilde{\boldsymbol q},\dot{\tilde{\boldsymbol q}})$. This study relies on the use of the feature established in (19) for the residual robot dynamics and the inequality $\|\boldsymbol f(\tilde{\boldsymbol q})\|\geq\delta\,\mathrm{sat}(\|\tilde{\boldsymbol q}\|;\alpha)$ from (25). First we study $-\dot{\tilde{\boldsymbol q}}^T\boldsymbol h(\tilde{\boldsymbol q},\dot{\tilde{\boldsymbol q}})$:

$$-\dot{\tilde{\boldsymbol q}}^T\boldsymbol h(\tilde{\boldsymbol q},\dot{\tilde{\boldsymbol q}})\leq\left\|\dot{\tilde{\boldsymbol q}}\right\|\left\|\boldsymbol h(\tilde{\boldsymbol q},\dot{\tilde{\boldsymbol q}})\right\|$$
$$\leq k_{C1}\|\dot{\boldsymbol q}_d\|_{\mathrm M}\left\|\dot{\tilde{\boldsymbol q}}\right\|^2+\delta\left\|\dot{\tilde{\boldsymbol q}}\right\|\mathrm{sat}(\|\tilde{\boldsymbol q}\|;\alpha)$$
$$\leq k_{C1}\|\dot{\boldsymbol q}_d\|_{\mathrm M}\left\|\dot{\tilde{\boldsymbol q}}\right\|^2+\left\|\dot{\tilde{\boldsymbol q}}\right\|\|\boldsymbol f(\tilde{\boldsymbol q})\|.\qquad(36)$$

The remaining term satisfies

$$-\varepsilon\boldsymbol f(\tilde{\boldsymbol q})^T\boldsymbol h(\tilde{\boldsymbol q},\dot{\tilde{\boldsymbol q}})\leq\varepsilon\|\boldsymbol f(\tilde{\boldsymbol q})\|\left\|\boldsymbol h(\tilde{\boldsymbol q},\dot{\tilde{\boldsymbol q}})\right\|$$
$$\leq\varepsilon k_{C1}\|\dot{\boldsymbol q}_d\|_{\mathrm M}\left\|\dot{\tilde{\boldsymbol q}}\right\|\|\boldsymbol f(\tilde{\boldsymbol q})\|$$
$$+\varepsilon\delta\|\boldsymbol f(\tilde{\boldsymbol q})\|\mathrm{sat}(\|\tilde{\boldsymbol q}\|;\alpha)$$
$$\leq\varepsilon k_{C1}\|\dot{\boldsymbol q}_d\|_{\mathrm M}\left\|\dot{\tilde{\boldsymbol q}}\right\|\|\boldsymbol f(\tilde{\boldsymbol q})\|+\varepsilon\|\boldsymbol f(\tilde{\boldsymbol q})\|^2.\qquad(37)$$

In view of the previous upper bounds (32)–(37), it is easy to recognize that the time derivative (31) of the Lyapunov function candidate holds

$$\dot V(\tilde{\boldsymbol q},\dot{\tilde{\boldsymbol q}})\leq-\begin{bmatrix}\|\dot{\tilde{\boldsymbol q}}\|\\\|\boldsymbol f(\tilde{\boldsymbol q})\|\end{bmatrix}^TQ\begin{bmatrix}\|\dot{\tilde{\boldsymbol q}}\|\\\|\boldsymbol f(\tilde{\boldsymbol q})\|\end{bmatrix}\qquad(38)$$

where the entries of matrix $Q$ are

$$Q_{11}=\lambda_{\mathrm m}\{K_v\}-\varepsilon\lambda_{\mathrm M}\{M\}\delta\frac{\alpha\sigma}{\tanh(\alpha\sigma)}$$
$$-\varepsilon k_{C1}\sqrt{n}\delta\frac{\alpha}{\tanh(\alpha\sigma)}-k_{C1}\|\dot{\boldsymbol q}_d\|_M,$$

$$Q_{12}=Q_{21}=-\frac{1}{2}[2\varepsilon k_{C1}\|\dot{\boldsymbol q}_d\|_{\mathrm M}+\varepsilon\lambda_{\mathrm M}\{K_v\}+1],$$

$$Q_{22}=\varepsilon\left[\frac{\lambda_{\mathrm m}\{K_p\}}{\delta}\frac{\tanh(\alpha\sigma)}{\alpha\sigma}-1\right].$$

https://doi.org/10.1017/S0263574700002848 Published online by Cambridge University Press

It only remains to find those conditions on $K_p$ and $K_v$ to ensure that $\dot{V}(\tilde{\boldsymbol{q}}, \dot{\tilde{\boldsymbol{q}}})$ is a negative definite function. In turn, this is guaranteed provided that $Q$ is a positive definite matrix. The following two conditions are necessary and sufficient to this end. The first condition is

$$\lambda_{\mathrm{m}}\{K_v\} > \varepsilon \left[ \lambda_{\mathrm{M}}\{M\}\delta \frac{\alpha\sigma}{\tanh(\alpha\sigma)} + k_{C1}\sqrt{n}\,\delta \frac{\alpha}{\tanh(\alpha\sigma)} \right] + k_{C1}\|\dot{\boldsymbol{q}}_d\|_{\mathrm{M}}. \tag{39}$$

The second condition results from imposing the determinant of $Q$ be strictly positive, thus

$$\lambda_{\mathrm{m}}\{K_p\} > \delta \frac{\alpha\sigma}{\tanh(\alpha\sigma)} \left[ 1 + \frac{[2\varepsilon k_{C1}\|\dot{\boldsymbol{q}}_d\|_{\mathrm{M}} + \varepsilon\lambda_{\mathrm{M}}\{K_v\} + 1]^2}{4\varepsilon[\lambda_{\mathrm{m}}\{K_v\} - \varepsilon\lambda_{\mathrm{M}}\{M\}\delta \frac{\alpha\sigma}{\tanh(\alpha\sigma)} - \varepsilon k_{C1}\sqrt{n}\,\delta \frac{\alpha}{\tanh(\alpha\sigma)} - k_{C1}\|\dot{\boldsymbol{q}}_d\|_{\mathrm{M}}]} \right] \tag{40}$$

However, according to definition (24), the constant $\varepsilon$ can be chosen arbitrarily small. Therefore, we expect that (40) can always be satisfied if

$$\lambda_{\mathrm{m}}\{K_p\} >> \delta \frac{\alpha\sigma}{\tanh(\alpha\sigma)}. \tag{41}$$

Since $\sigma > 0$ can be chosen arbitrarily small, then invoking

$$\lim_{\sigma \to 0} \frac{\alpha\sigma}{\tanh(\alpha\sigma)} = 1,$$

we obtain condition (13) $\lambda_{\mathrm{m}}\{K_p\} >> \delta$.

On the other hand, condition (14) $\lambda_{\mathrm{m}}\{K_v\} > k_{C1}\|\dot{\boldsymbol{q}}_d\|_{\mathrm{M}}$ ensures that (39) holds by choosing $\varepsilon$ sufficiently small.

Thus we have shown that $\dot{V}(\tilde{\boldsymbol{q}}, \dot{\tilde{\boldsymbol{q}}})$ is a globally negative definite function. Using this fact together with the positive definiteness in a global sense of the Lyapunov function candidate, we conclude that, under selection of $K_p$ and $K_v$ given by (39)–(40), the origin of the state space $[\tilde{\boldsymbol{q}}^T\ \dot{\tilde{\boldsymbol{q}}}^T]^T = 0 \in \mathbb{R}^{2n}$ is a globally asymptotically stable equilibrium of the closed-loop system (15).

## 6. EXPERIMENTAL EVALUATION

The experimental system consists of a direct-drive vertical arm with two degrees-of-freedom whose rigid links are joined with revolute joints (see Figure 3).

It is equipped with position sensors, motor drivers, a Digital Signal Processor (DSP) motion control board, a host computer 486 PC and software environment which generates a user-friendly interface.

Considering the values of the physical parameters of our robot arm, we have the following entries of the robot dynamics:[20]

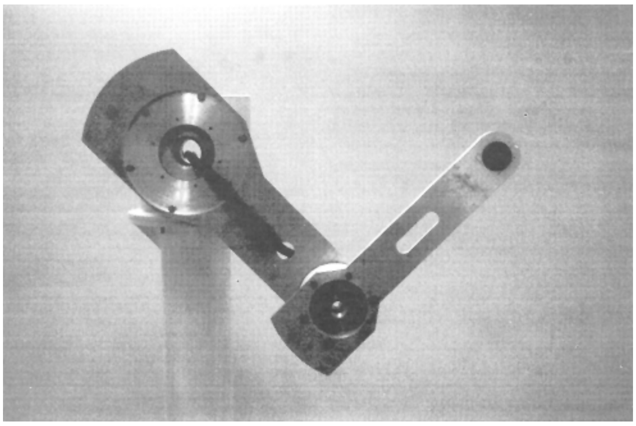

Fig. 3. Experimental arm.

$$M(\boldsymbol{q}) = \begin{bmatrix} 2.351 + 0.168\cos(q_2) & 0.102 + 0.084\cos(q_2) \\ 0.102 + 0.084\cos(q_2) & 0.102 \end{bmatrix}, \tag{42}$$

$$C(\boldsymbol{q}, \dot{\boldsymbol{q}}) = \begin{bmatrix} -0.168\sin(q_2)\,\dot{q}_2 & -0.084\sin(q_2)\,\dot{q}_2 \\ 0.084\sin(q_2)\,\dot{q}_1 & 0 \end{bmatrix}, \tag{43}$$

$$\boldsymbol{g}(\boldsymbol{q}) = 9.81 \begin{bmatrix} 3.921\sin(q_1) + 0.186\sin(q_1 + q_2) \\ 0.186\sin(q_1 + q_2) \end{bmatrix}. \tag{44}$$

This information is important to evaluate the following parameters using (7)–(10):

$$k_M = 0.672\ \mathrm{kg\ m}^2; \quad k_{C_1} = 0.336\ \mathrm{kg\ m}^2 \tag{45}$$

$$k_{C_2} = 0.672\ \mathrm{kg\ m}^2; \quad k_g = 80.578\ \mathrm{kg\ m}^2/\mathrm{sec}^2 \tag{46}$$

$$k_1 = 40.33\ \mathrm{kg\ m}^2/\mathrm{sec}^2; \quad k_2 = \lambda_{\mathrm{M}}\{M\} = 2.533\ \mathrm{kg\ m}^2. \tag{47}$$

### 6.1 *Desired position trajectory*

The desired position trajectory should be chosen to exhibit motion profile without abrupt changes in position, velocity and acceleration from the beginning to the end of the motion, as well as generating fast rigid dynamics dominated behavior, while preventing the actuators from saturating. The structure of the desired trajectory we have used is similar to those proposed in References 21–23, that is

$$\boldsymbol{q}_d(t) = \begin{bmatrix} 0.7854[1 - e^{-2.0\,t^3}] + 0.1745[1 - e^{-2.0\,t^3}]\sin(\omega_1 t) \\ 1.0472[1 - e^{-1.8\,t^3}] + 2.1816[1 - e^{-1.8\,t^3}]\sin(\omega_2 t) \end{bmatrix} [\mathrm{rad}]$$

https://doi.org/10.1017/S0263574700002848 Published online by Cambridge University Press

where $\omega_1 = 15$ rad/sec and $\omega_2 = 3.5$ rad/sec. This desired trajectory is sufficient to produce a larger excursion in the applied torque signals exploiting widely the actuator capabilities. Also, it requests velocity and acceleration peaks as large as $|\dot{q}_{d_1}| = 2.61$ rad/sec and $|\dot{q}_{d_2}| = 7.63$ rad/sec, $|\ddot{q}_{d_1}| = 39.26$ rad/sec$^2$ and $|\ddot{q}_{d_2}| = 26.72$ rad/sec$^2$ for the shoulder and elbow joints respectively.

### 6.2 *Selection of gains*

Using the numerical values of $k_M$, $k_{C_1}$, $k_{C_2}$, $k_g$, $k_1$, $k_2$, given in (45)–(47), and employing $\|\dot{\boldsymbol{q}}_d\|_M = 8.07$ rad/sec., and $\|\ddot{\boldsymbol{q}}_d\|_M = 47.49$ rad/sec$^2$, we obtain the following numerical values of

$$\alpha = 2.34$$
$$\delta = 156.25 \text{ kg m}^2/\text{sec}^2.$$

The maximum eigenvalue of the inertia matrix (42), given in (47), and the numerical values of $\varepsilon = 0.005$ and $\sigma = 0.1$ –fulfilling (24)–, are also used to obtain the selection condition for $K_v$, in agreement with (39), as:

$$\lambda_m\{K_v\} > 8.506 \text{ N m sec/rad.} \tag{48}$$

Once, we know the minimum bound of $\lambda_m\{K_v\}$ we proceed to fix $\lambda_m\{K_v\}$ and $\lambda_M\{K_v\}$, in accordance with (48). After some experimental tests we chose

$$\lambda_m\{K_v\} = 50 \text{ N m sec/rad,} \tag{49}$$

$$\lambda_M\{K_v\} = 150 \text{ N m sec/rad.} \tag{50}$$

We are now ready to compute the allowed minimum bound of $\lambda_m\{K_p\}$ according to (40), whose numerical value resulted in

$$\lambda_m\{K_p\} > 764.5 \text{ N m/rad,} \tag{51}$$

During the preliminary experiments we first tested several $K_p$ and $K_v$ gains for the controller in agreement to (48) and (51) and such as to avoid saturating the actuators. The controller gains $K_p$ and $K_v$ were finally set to

$$K_p = \text{diag}\{2000, 1000\} \text{ N m/rad,} \tag{52}$$

$$K_v = \text{diag}\{150, 50\} \text{ N m sec/rad.} \tag{53}$$

### 6.3 *Experimental results*

Three control schemes were tested in our experimental set-up. In all cases the initial configuration of the robot arm was in its equilibrium position at $q_1(0) = q_2(0) = 0$. During experiments, the controllers incorporated compensation for viscous friction into the control laws.

The first experiment was conducted using the PD control with gravity compensation described by

$$\tau = K_p\tilde{\boldsymbol{q}} + K_v\dot{\tilde{\boldsymbol{q}}} + \boldsymbol{g}(\boldsymbol{q}) \tag{54}$$

with the proportional and derivative matrices given in (52)–(53). This is a simple controller which requires only the knowledge of a portion of the dynamic model, namely the gravitational torque vector $\boldsymbol{g}(\boldsymbol{q})$. It can be shown that for a nonvanishing time varying desired joint position, this control scheme cannot ensure asymptotic joint position

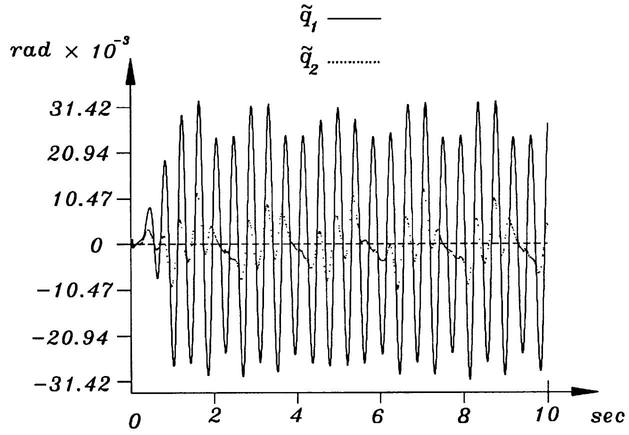


Fig. 4. Tracking errors for the PD controller.

tracking. The components of the position error obtained from experiments are shown in Figure 4 which will serve as reference for comparison with results obtained using full model-based controllers.

The PD control with feedforward compensation (2) was the second controller tested on the direct-drive arm. Observe that in contrast with the simple PD control with gravity compensation (54), it compensates for the full robot dynamics evaluated at the desired motion trajectory. From this fact we expect a better control system performance. This is confirmed from the position error shown in Figure 5 where the full feedforward compensation has reduced the peak tracking error significantly when compared to the PD control with gravity compensation.

The third controller tested was the computed torque control method given by

$$\tau = M(\boldsymbol{q})[\ddot{\boldsymbol{q}}_d + K_v\dot{\tilde{\boldsymbol{q}}} + K_p\tilde{\boldsymbol{q}}] + C(\boldsymbol{q}, \dot{\boldsymbol{q}})\dot{\boldsymbol{q}} + \boldsymbol{g}(\boldsymbol{q}).$$

The position error obtained with the computed-torque controller is depicted in Figure 6. Visual examination of Figures 5 and 6 allows the conclusion that the PD control with feedforward compensation performs as well as the computed torque control scheme which is perhaps the paradigm of model-based manipulator motion control. The remaining position error observed in Figures 5 and 6 are mainly due to uncompensated Coulomb friction.

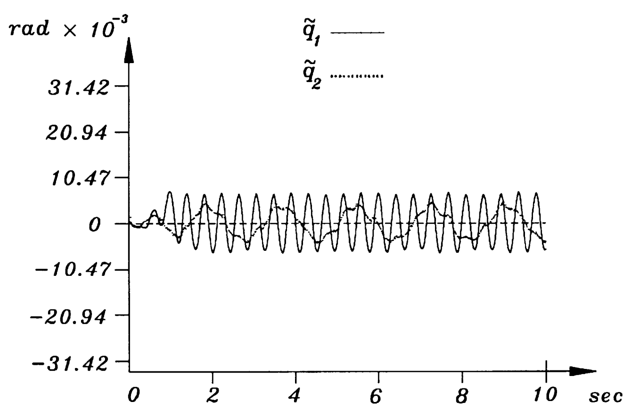


Fig. 5. Tracking errors for PD control with feedforward compensation.

https://doi.org/10.1017/S0263574700002848 Published online by Cambridge University Press

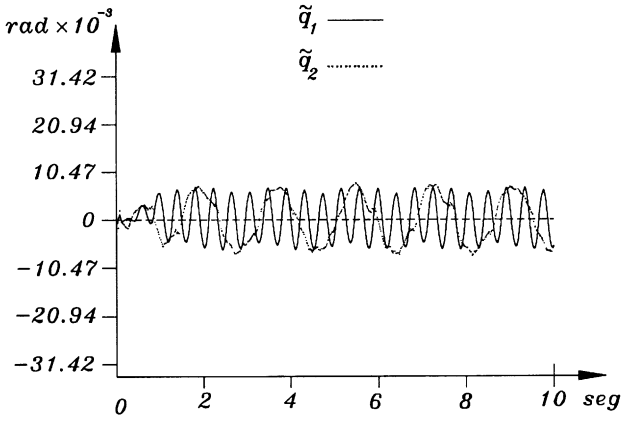


Fig. 6. Tracking errors for computed torque control.

## 7. CONCLUSION

This paper has presented a novel analysis of the PD control with feedforward compensation of robot manipulators. To this end, we have proposed a strict Lyapunov function which has allowed to obtain, for the first time, conditions on the controller gains to ensure global asymptotic stability. This was possible thanks to a new manner to describe growth rates of the residual robot dynamics. The paper also introduced an alternative way to derive conditions on the proportional gain matrix for equilibrium uniqueness. Finally, the effectiveness of the PD control with feedforward compensation has been illustrated through experiments on a direct-drive robot arm.

## ACKNOWLEDGEMENT

The authors would like to thank Prof. Fernando Reyes for his help during experimental tests.

## APPENDIX A

This appendix is devoted to establish a useful lemma to describe growth rate of important terms of the dynamics (1). Also, the proof of the upper bound on the residual robot dynamics (19) is presented.

With reference to definition (20) of the hard saturation function shown in Figure 2, the following two useful features of the hard saturation function can be extracted. Function sat($x$; $k$) is bounded independently of $x$, i.e. for any $a>0$

$$a\ \mathrm{sat}(|x|;k) \le ak \quad \forall\, x \in \mathbb{R}.$$

On the other hand, saturation function sat($|x|$; $k$) can be upper bounded by a linear function of $|x|$ regardless $k$, i.e. for any $a>0$

$$a\ \mathrm{sat}(|x|;k) \le a|x| \quad \forall\, x \in \mathbb{R}$$

Therefore, for a function $f:\mathbb{R}\to\mathbb{R}$, the following equivalence holds for all $x \in \mathbb{R}$

$$\left\{\begin{array}{l} |f(x)| \le ak \\ |f(x)| \le a|x| \end{array}\right. \Leftrightarrow |f(x)| \le a\ \mathrm{sat}(|x|;k) \qquad (55)$$

The saturation function sat($x$; $k$) is suitable to describe growth rate of important terms of the dynamics (1). This is stated in the following

***Lemma A.*** Consider the robot dynamics (1). Then, for all $\boldsymbol{\upsilon}$, $\boldsymbol{w}$, $\boldsymbol{x}$, $\boldsymbol{y}$, $\boldsymbol{z} \in \mathbb{R}^n$ we have

1. $\|\boldsymbol{g}(\boldsymbol{x})-\boldsymbol{g}(\boldsymbol{y})\| \le k_g\ \mathrm{sat}(\|\boldsymbol{x}-\boldsymbol{y}\|;\ 2k_1/k_g)$.
2. $\|C(\boldsymbol{x},\boldsymbol{z})\boldsymbol{w}-C(\boldsymbol{y},\boldsymbol{\upsilon})\boldsymbol{w}\| \le k_{C1}\|\boldsymbol{z}-\boldsymbol{\upsilon}\|\ \|\boldsymbol{w}\| + K_{C2}\|\boldsymbol{z}\|\ \|\boldsymbol{w}\|\ \mathrm{sat}(\|\boldsymbol{x}-\boldsymbol{y}\|;\ 2k_{C1}/k_{C2})$.
3. $\|M(\boldsymbol{x})\boldsymbol{z}-M(\boldsymbol{y})\boldsymbol{z}\| \le k_M\ \|\boldsymbol{z}\|\ \mathrm{sat}(\|\boldsymbol{x}-\boldsymbol{y}\|;\ 2k_2/k_M)$.

∇∇∇

***Proof:*** From (5) and (11) we notice that $\boldsymbol{g(q)}$ satisfies simultaneously

$$\|\boldsymbol{g}(\boldsymbol{x})-\boldsymbol{g}(\boldsymbol{y})\| \le k_g\|\boldsymbol{x}-\boldsymbol{y}\|$$

and

$$\|\boldsymbol{g}(\boldsymbol{x})-\boldsymbol{g}(\boldsymbol{y})\| \le 2k_1$$

for all $\boldsymbol{x}$, $\boldsymbol{y} \in \mathbb{R}^n$, hence result 1 of lemma follows immediately from (55).

On the other hand, it follows from (4) that $C(\boldsymbol{q},\dot{\boldsymbol{q}})$ carries out

$$\begin{aligned}\|[C(\boldsymbol{x},\boldsymbol{z})-C(\boldsymbol{y},\boldsymbol{\upsilon})]\boldsymbol{w}\| \le\ & k_{C1}\|\boldsymbol{z}-\boldsymbol{\upsilon}\|\ \|\boldsymbol{w}\| \\ &+ k_{C2}\|\boldsymbol{z}\|\ \|\boldsymbol{x}-\boldsymbol{y}\|\ \|\boldsymbol{w}\| \end{aligned} \qquad (56)$$

for all $\boldsymbol{x}$, $\boldsymbol{y}$, $\boldsymbol{\upsilon}$, $\boldsymbol{w} \in \mathbb{R}^n$. But it is also right that the left hand side satisfies

$$\|[C(\boldsymbol{x},\boldsymbol{z})-C(\boldsymbol{y},\boldsymbol{\upsilon})]\boldsymbol{w}\| \le \|C(\boldsymbol{x},\boldsymbol{z})\boldsymbol{w}\| + \|C(\boldsymbol{y},\boldsymbol{\upsilon})\boldsymbol{w}\|$$

which yields

$$\|[C(\boldsymbol{x},\boldsymbol{z})-C(\boldsymbol{y},\boldsymbol{\upsilon})]\boldsymbol{w}\| \le k_{C1}\|\boldsymbol{z}-\boldsymbol{\upsilon}\|\ \|\boldsymbol{w}\| + 2k_{C1}\|\boldsymbol{z}\|\ \|\boldsymbol{w}\| \qquad (57)$$

because in virtue of (6) we have

$$\|C(\boldsymbol{x},\boldsymbol{z})\boldsymbol{w}\| \le k_{C1}\ \|\boldsymbol{z}\|\ \|\boldsymbol{w}\|$$

and

$$\begin{aligned}\|C(\boldsymbol{y},\boldsymbol{\upsilon})\boldsymbol{w}\| &\le k_{C1}\ \|\boldsymbol{\upsilon}\|\ \|\boldsymbol{w}\| \\ &= k_{C1}\ \|\boldsymbol{z}-\boldsymbol{z}+\boldsymbol{\upsilon}\|\ \|\boldsymbol{w}\| \\ &\le k_{C1}\ \|\boldsymbol{z}\|\ \|\boldsymbol{w}\| + k_{C1}\|\boldsymbol{z}-\boldsymbol{\upsilon}\|\ \|\boldsymbol{w}\|.\end{aligned}$$

Hence, result 2 of lemma A is obtained straightforward considering both (56) and (57), together with (55).

In order to prove result 3, we recall from (3) that

$$\|M(\boldsymbol{x})\boldsymbol{z}-\boldsymbol{M}(\boldsymbol{y})\boldsymbol{z}\| \le k_M\|\boldsymbol{x}-\boldsymbol{y}\|\ \|\boldsymbol{z}\|.$$

It is also true – applying (12) – that

$$\|M(\boldsymbol{x})\boldsymbol{z}-M(\boldsymbol{y})\boldsymbol{z}\| \le 2\|M(\boldsymbol{x})\boldsymbol{z}\| \le 2k_2\ \|\boldsymbol{z}\|$$

for all $\boldsymbol{x}$, $\boldsymbol{y}$, $\boldsymbol{z} \in \mathbb{R}^n$. Finally, the desired result follows from (55).

□□□

The remaining deals with the proof of (19). The residual robot dynamics was defined in (16). Utilizing lemma A, it is easy to show that the norm of the residual dynamics satisfies

$$\begin{aligned}\|\boldsymbol{h}(\tilde{\boldsymbol{q}},\dot{\tilde{\boldsymbol{q}}})\| \le\ & \|[M(\boldsymbol{q}_d)-M(\boldsymbol{q})]\ddot{\boldsymbol{q}}_d\| + \|[C(\boldsymbol{q}_d,\dot{\boldsymbol{q}}_d) \\ & - C(\boldsymbol{q},\dot{\boldsymbol{q}})]\dot{\boldsymbol{q}}_d\| + \|\boldsymbol{g}(\boldsymbol{q}_d)-\boldsymbol{g}(\boldsymbol{q})\| \\ \le\ & k_M\|\ddot{\boldsymbol{q}}_d\|_M\ \mathrm{sat}(\|\tilde{\boldsymbol{q}}\|;\ 2k_2/k_M) \\ & + k_{C1}\|\dot{\boldsymbol{q}}_d\|_M\|\dot{\tilde{\boldsymbol{q}}}\| \\ & + k_{C2}\|\dot{\boldsymbol{q}}_d\|_M^2\ \mathrm{sat}(\|\tilde{\boldsymbol{q}}\|;\ 2k_{C1}/k_{C2}) \\ & + k_g\ \mathrm{sat}(\|\tilde{\boldsymbol{q}}\|;\ 2k_1/k_g).\end{aligned}$$

https://doi.org/10.1017/S0263574700002848 Published online by Cambridge University Press

Finally, the definition of the saturation function (20) leads to the desired result:

$$\|\boldsymbol{h}(\tilde{\boldsymbol{q}}, \dot{\tilde{\boldsymbol{q}}})\| \leq k_{C1}\|\dot{\boldsymbol{q}}_d\|_M \|\dot{\tilde{\boldsymbol{q}}}\| + [k_g + k_M\|\ddot{\boldsymbol{q}}_d\|_M + k_{C2}\|\dot{\boldsymbol{q}}_d\|_M^2] \ \mathrm{sat}(\|\tilde{\boldsymbol{q}}\|; \alpha)$$

where $\alpha$ was defined in (17) in such a way that the maximum value of the saturation function be the sum of each maximum values of the individual saturation functions.

## References


1. M.W. Spong and M. Vidyasagar, *Robot Dynamics and Control*, (John Wiley and Sons, New York, 1989).
2. A. Liégeois, A. Fournier and M.J. Aldon, "Model reference control of high-velocity industrial robots", *Proc. of the Joint Automatic Control Conference*, San Francisco, CA., (August, 1980). Session TP10 – D no numbered pages.
3. H. Asada, T. Kanade and I. Takeyama, "Control of a direct-drive arm", *ASME Journal of Dynamic Systems, Measurement, and Control*, **105**, 136–142 (1983).
4. H. Asada and K. Youcef-Toumi, *Direct-drive Robots*, (The MIT Press, 1987).
5. C.H. An, C.G. Atkeson and J.M. Hollerbach, "Experimental determination of the effect of feedforward control on trajectory tracking errors", *Proc. IEEE International Conference on Robotics and Automation*, San Francisco, CA (April, 1996) pp. 55–60.
6. C.H. An, C.G. Atkeson and J.M. Hollerbach, *Model-Based Control of a Robot Manipulator* (The MIT Press, 1988).
7. C.H. An, C.G. Atkeson, J.D. Griffiths and J.M. Hollerbach, "Experimental evaluation of feedforward and computed torque control", *IEEE Trans. on Robotics and Automation*, **5**, No. 3, 368–373 (June, 1989).
8. P.K. Khosla and T. Kanade, "Experimental evaluation of nonlinear feedback and feedforward control schemes for manipulators", *Int. J. Robotics Research* **7**, No. 1, 18–28 (February, 1988).
9. P.K. Khosla and T. Kanade, "Real-Time implementation and evaluation of computed-torque scheme", *IEEE Trans. on Robotics and Automation*, **5**, No. 2, 245–252 (April, 1989).
10. H.T. Chen, P. Jiang, W.H. Zhu and Y.J. Wang, "Comparative study of D. D. robot control algorithms for trajectory tracking", *12th IFAC World Congress*, Sydney, Australia (July, 1993) **Vol. 6**, pp. 157–160.
11. Z. Lu, K.B. Shimoga and A.A. Goldenberg, "Experimental determination of dynamic parameters of robotic arms", *J. of Robotic Systems*, **10**, No. 8, 1009–1029 (1993).
12. F. Caccavale and P. Chiacchio, "Identification of dynamic parameters and feedforward control for a conventional industrial manipulator", *Control Engineering Practice*, **2**, No. 6, 1039–1050 (1994).
13. T.J. Tarn, A.K. Bejczy, G.T. Marth and A.K. Ramadarai, "Performance comparison of four manipulators servo schemes", *IEEE Control System*, **13**, No. 1, 22–29 (February, 1993).
14. J.T. Wen and D.S. Bayard, "New class of control laws for robotic manipulators. Part 1: Non-adaptive case", *Int. J. Control*, **47**, No. 5, 1361–1385 (1988).
15. J.T. Wen, "A unified perspective on robot control: The energy Lyapunov function approach", *Int. J. Adaptive Control and Signal Processing*, **4**, No. 6, 487–500 (November–December, 1990).
16. R. Kelly and R. Salgado, "PD control with computed feedforward of robot manipulators: A design procedure", *IEEE Transactions on Robotics and Automation*, **10**, No. 4, pp. 566–571 (August, 1994).
17. S. Arimoto, "Fundamental problems of robot control: Part I. Innovations in the realm of robot servo–loops", *Robotica*, **13**, Part 1, 19–27, (1995).
18. S. Arimoto, "Fundamental problems of robot control: Part II. A nonlinear circuit theory towards an understanding of dexterous motions", *Robotica*, **13**, Part 2, 111–122 (1995).
19. D. Koditschek, "Natural motion for robot arms", *Proc. of the 1984 IEEE Conf. on Decision and Control*, Las Vegas, NV. (1984) pp. 733–735.
20. F. Reyes and R. Kelly, "Experimental evaluation of identification schemes on a direct drive robot", *Robotica*, **15**, 563–571 (September–October, 1997).
21. D.M. Dawson, J.J. Carroll and M. Schneider, "Integrator backstepping control of a brush dc motor turning a robotic load", *IEEE Transactions on Control System Technology*, **2**, No. 3, 233–244 (September, 1994).
22. M.S. de Queiroz, D. Dawson and T. Burg, "Reexamination of the DCAL controller for rigid link robots", *Robotica*, **14**, Part 1, 41–49 (1996).
23. W.E. Dixon, M.S. de Queiroz, F. Zhang and D.M. Dawson, "Tracking control of robot manipulators with bounded torque inputs", *Robotica*, **17**, No. 2, 121–129 (March–April, 1999).


https://doi.org/10.1017/S0263574700002848 Published online by Cambridge University Press